

Research Paper

In Silico Prediction of Drug Permeability Across Buccal Mucosa

Amit Kokate,¹ Xiaoling Li,¹ Paul J. Williams,² Parminder Singh,³ and Bhaskara R. Jasti^{1,4}

Received September 15, 2008; accepted January 12, 2009; published online January 30, 2009

Purpose. To develop and validate a computational model capable of predicting buccal permeability based on various structural and physicochemical descriptors.

Methods. Apparent permeability coefficients (K_p) of 15 different drugs across porcine buccal mucosa were determined. Multiple linear regression (MLR) and maximum likelihood estimations (MLE) were used to develop the model based on a training set of 15 drugs with permeability as the response variable and the various descriptors as the predictor variables. The final model was validated with an external data set consisting of permeability values obtained from the literature.

Results. Drug permeabilities ranged from 30×10^{-6} (nimesulide) to 3.3×10^{-9} cm/s (furosemide). Regression analysis showed that 95% of the variability in permeability data can be explained by a model that includes molecular volume, distribution coefficient at pH 6.8, number of hydrogen bond donors, and number of rotatable bonds. Smaller molecular size, high lipophilicity, lower hydrogen bond capability and greater flexibility were important for permeability. The buccal model was found to have a good predictive capability.

Conclusion. A simple model was developed and validated for predicting the buccal drug permeability. This model will be useful in assessing the feasibility of drugs for transbuccal delivery.

KEY WORDS: buccal; *in silico*; permeability; prediction

INTRODUCTION

The peroral and parenteral routes are commonly used for administration of drugs. However, the peroral route imposes limitations on the absorption of certain drugs owing to extensive first-pass metabolism and hydrolysis of acid-labile drugs. The parenteral route is inconvenient and suffers from patient acceptability due to its invasive nature. In addition, parenteral products need to be sterile and have a severe restriction on the concentration and type of excipients used. These limitations have led to the investigation of alternative routes for drug delivery such as the buccal route. Drugs delivered by the buccal route gain direct entry into the systemic circulation. The gastric digestive fluids and first-pass metabolism in the gastrointestinal tract are thereby avoided (1). The permeability of the buccal mucosa is four to 4,000 times greater than the permeability across skin. As a result, a faster onset of action for several drugs is observed (2). A shorter turnover time in the oral mucosa (14 days) as opposed to skin (27 days) ensures a faster recovery of the oral mucosa (3). In addition, drug delivery across this tissue offers several

other advantages such as good accessibility for administering drugs and removal of delivery devices in case of an emergency.

Structurally, oral mucosa is closer to skin than gastrointestinal mucosa. Both skin and oral mucosa have a stratified (multilayered) squamous epithelium, whereas, the intestine is lined by a simple, columnar epithelium (4). The epithelium forms the rate-limiting barrier to absorption across this membrane (5). The buccal epithelium has a surface area of 50 cm² and a thickness of 500–600 μm (6). The lipid and glycolipid content extruded from the membrane-coating granules (MCGs) in the intercellular space ensures cohesion of the epithelial cells. The intercellular space is filled with about 50% polar lipids such as phospholipids and glycosylceramides (7). Based on the biochemical composition and structure of the buccal mucosa, drugs can permeate by the lipoidal and/or aqueous pathways. The lipoidal pathway encompasses both transcellular transport and transport through the intercellular lipids by partitioning. The water molecules entrapped by the polar head groups of intercellular lipids result in an aqueous pathway (8).

Porcine buccal mucosa is similar to that of human in terms of structure, composition and permeability to a greater extent than any other animal (7). As a result, *in vitro* permeation studies across porcine buccal mucosa are commonly used to estimate human buccal absorption (9). However, these studies are limited by availability of fresh tissues apart from being time-consuming and labor-intensive. *In silico* prediction of buccal permeability is an alternative to experimental permeation studies. At present, there is no simple model capable of predicting buccal permeability of a wide range of small

¹Department of Pharmaceutics and Medicinal Chemistry, Thomas J. Long School of Pharmacy and Health Sciences, University of the Pacific, Stockton, California 95211, USA.

²Department of Pharmacy Practice, Thomas J. Long School of Pharmacy and Health Sciences, University of the Pacific, Stockton, California 95211, USA.

³Corium International, Menlo Park, California 94025, USA.

⁴To whom correspondence should be addressed. (e-mail: bjasti@pacific.edu)

molecular drugs. This has led to the use of existing transdermal models such as the Potts–Guy (PG) model (10) for predicting buccal permeability due to the greater structural and biochemical proximity of buccal mucosa to skin than other tissues such as intestine. However, use of such models is inadequate as the permeation of ionized drug species is significant in the buccal mucosa and distribution coefficient ($\log D$) was found to correlate better to the buccal permeability as opposed to $\log P$ that was proposed in the existing models.

Drug permeability across a biological membrane depends on the properties of the barrier and permeant. Various structural and physicochemical parameters such as, size, charge, lipophilicity, and hydrogen-bonding capacity influence the permeability of a molecule across a membrane (11). The objective of this study was to develop a computational model capable of predicting buccal drug permeability based on molecular descriptors. A wide variation in the experimental conditions reported in literature might lead to large differences in permeability values of a drug. As a result, permeabilities of 15 different drugs under controlled experimental conditions were determined as a part of this work.

MATERIALS AND METHODS

Materials

Nimesulide was purchased from Alexis Biochemicals (Lausen, Switzerland). The remaining drugs (bupivacaine HCl, lidocaine HCl, propranolol HCl, atenolol, caffeine, antipyrine, furosemide, verapamil HCl, diltiazem HCl, amitriptyline HCl, naproxen, warfarin, metoprolol, and pindolol) were purchased from Sigma Chemicals (St. Louis, MO). HPLC grade solvents were purchased from Fisher Scientific (Bridgewater, NJ). All other reagents were of analytical grade and used as received. Deionized water was used in preparing the buffers and drug donor solutions. Drug dissolved/suspended in phosphate buffer (pH 6.8) was used as the donor solution whereas phosphate buffer (pH 7.4) was used as the receiver solution during the permeation studies.

Drugs and Descriptors

The 15 drugs used in developing the model covered a wide range for each descriptor. These compounds were structurally diverse and stable under the experimental conditions. The model drugs used in this study included four acidic (furosemide, naproxen, warfarin, nimesulide), nine basic (lidocaine, propranolol, atenolol, bupivacaine, verapamil, diltiazem, amitriptyline, metoprolol, pindolol), and two neutral (caffeine, antipyrine) molecules (Fig. 1).

The various descriptors used in this study were molecular weight (MW), molecular volume (MV), octanol–water partition coefficient ($\log P$), $\log D_{6.8}$ (logarithm of distribution coefficient at pH 6.8, which corresponds to salivary pH), polar surface area (TPSA), number of hydrogen bond acceptors (HBA) and donors (HBD), number of rotatable bonds (nRotB), solubility (at pH 6.8), and melting point (mp). Solubility was determined experimentally using the shake-flask method. $\log P$, $\log D_{6.8}$ and mp were obtained from

the literature. The remaining descriptors were calculated using Molinspiration®, which is an online cheminformatics service (12). The MV calculations in Molinspiration® are based on the group contribution approach in which, 3D molecular geometries fully optimized by the semi-empirical AM1 method were obtained for a training set containing about 12,000 drug-like molecules. The sum of fragment contributions was then fit to these “real” 3D volumes. An excellent fit with an R^2 of 1.000 was obtained between the 2D- and 3D-volumes (12). Also, this program uses a new, simple, and drastically fast approach for the calculation of polar surface area or topological polar surface area (TPSA). The TPSA approach is based on the summation of tabulated surface contributions of polar fragments. The polar fragment contributions were previously determined by fitting the fragment based TPSA (for 43 different polar atom types) to the single conformer 3D PSA for 34,810 drugs from the World Drug Index by the least-squares method (13). A very good correlation ($R^2=0.982$) was obtained between the TPSA and 3D PSA.

In addition to MV and TPSA, Molinspiration® can also be used for calculation of other molecular properties including the number of hydrogen-bond acceptors (HBA) and donors (HBD) and number of rotatable bonds (nRotB). HBA and HBD are calculated based on the number of oxygen and nitrogen atoms and the number of hydrogen atoms connected to nitrogen and oxygen atoms, respectively in a molecule. The nRotB is defined as “any single bond, not in a ring, bound to a non-terminal heavy (i.e., non-hydrogen) atom.” C–N bonds are excluded due to a high rotational energy barrier (14). The values for the various descriptors for each drug are given in Table I. The values for the descriptors were obtained from various sources (15–29).

Solubility Determination

The solubility of various drugs was determined in Phosphate buffer, pH 6.8 by the shake-flask method. Excess amount of drug was added to the buffer in a scintillation vial. The contents of the scintillation vial were sonicated for 0.5 h to disperse the drug particles followed by stirring in a 37°C walk-in incubator. The pH was readjusted to the desired value with either sodium hydroxide (0.1 N) or phosphoric acid (0.1 N) solution depending on the drug. A sample was withdrawn after 48 h and filtered through a 0.2 μm nylon filter (Fisherbrand®, Fisher Scientific, PA) followed by dilution with buffer. Drug samples were stored under refrigerated conditions until further analysis by HPLC. All experiments were conducted in triplicate.

Tissue Preparation

Porcine buccal tissue was obtained from a local ranch immediately after the pigs were sacrificed. The tissues were stored in phosphate buffer, pH 7.4 during transport and processing. Buccal epithelium was separated from the underlying connective tissue by trimming the latter to a thickness of $500 \pm 50 \mu\text{m}$. This thickness corresponds to buccal epithelial thickness, which contributes to the diffusional barrier (6). Permeation studies were initiated within 2 h of the pigs sacrifice. In general, all replicate permeability studies for a

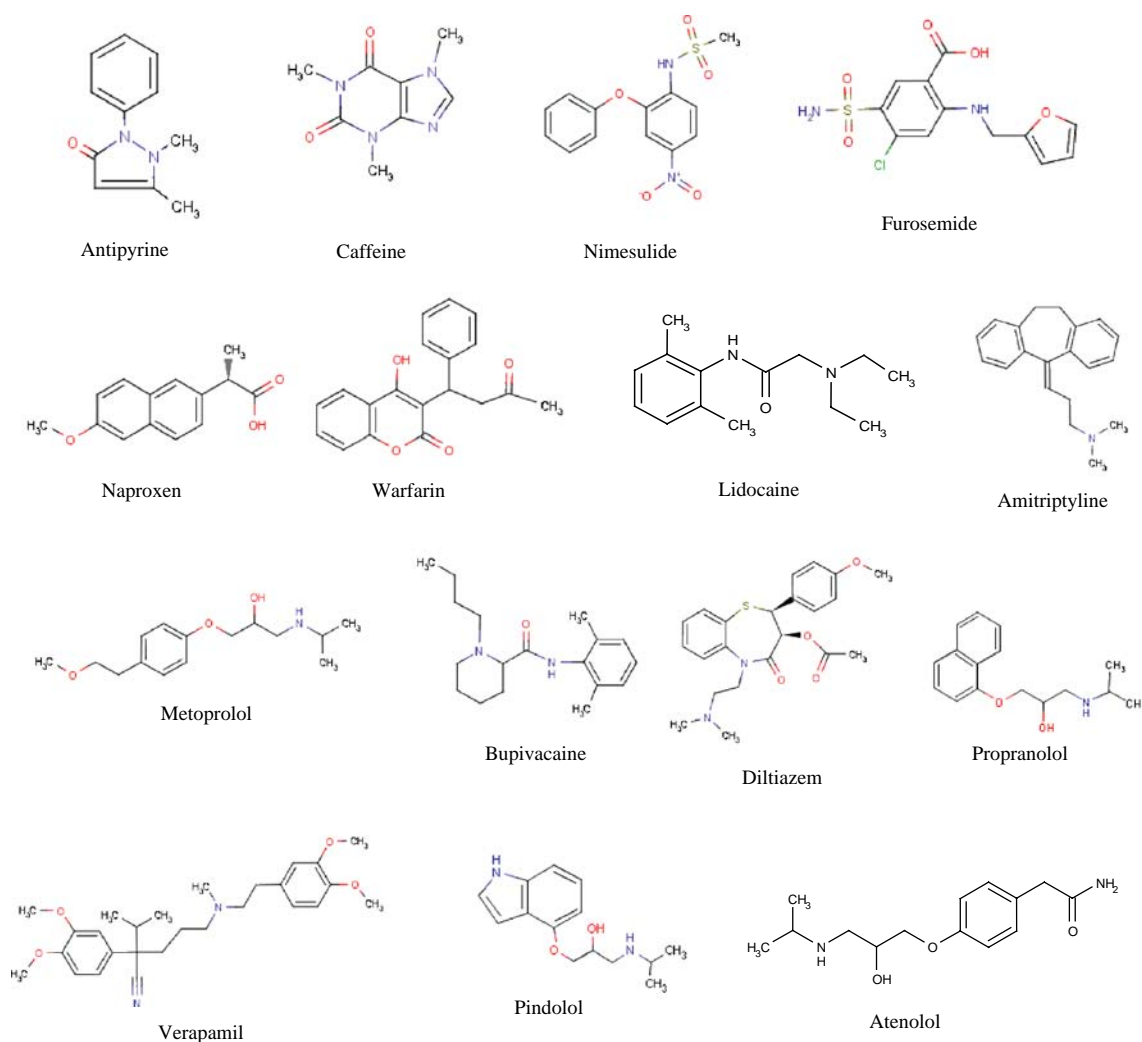


Fig. 1. Structures of various drugs used in developing the model.

Table I. Molecular Descriptor Values for the Various Drugs Used in this Study

Drug	pK _a	MW	MV	TPSA	HBA	HBD	nRotB	logP	logD (6.8)	mp (°C)	Sol (mM)	Ref
Lidocaine	7.90 (B)	234	245	32	3	1	5	2.10	1.20	69	251.7	(15–18)
Propranolol	9.45 (B)	259	258	41	3	2	6	3.48	1.20	96	1208.7	(19–21)
Atenolol	9.54 (B)	266	261	85	5	4	8	0.22	-1.30	147	–	(16,19, 21)
Verapamil	8.90 (B)	455	454	64	6	0	13	3.79	1.72	25	3.2	(16,22,23)
Diltiazem	7.70 (B)	415	378	59	6	0	7	2.79	1.04	–	4.8	(16,23)
Amitriptyline	9.31 (B)	277	285	3	1	0	3	5.04	1.64	–	12.5	(16)
Bupivacaine	8.10 (B)	288	302	32	3	1	5	3.70	2.48	108	4.0	(15,16)
Metoprolol	9.56 (B)	267	273	51	4	2	9	1.95	-0.56	35	–	(21,24)
Pindolol	9.54 (B)	248	243	57	4	3	6	1.83	-0.90	172	–	(21)
Nimesulide	6.50 (A)	308	248	101	7	1	5	1.94	1.69	147	0.1	(16,25)
Furosemide	4.70 (A)	331	250	123	7	4	5	2.03	-1.00	206	68.3	(19,22)
Naproxen	4.20 (A)	230	214	47	3	1	3	3.18	0.60	152	96.7	(16,18)
Warfarin	4.90 (A)	308	277	68	4	1	4	2.60	0.70	163	3.9	(16)
Caffeine	N	194	168	62	6	0	0	-0.07	-0.07	238	137.6	(26)
Antipyrine	N	188	178	27	3	0	1	0.39	0.39	114	5851.1	(27)

mp for most drugs was obtained from Merck Index (28) and ChemIDplus (16). Solubilities of atenolol, metoprolol and pindolol were not considered as they were extremely high. Diltiazem and amitriptyline (free base) are liquids at room temperature
A acidic drug, *B* basic drug, *N* neutral drug

particular drug were performed using membrane specimens obtained from either one or two animals.

Permeation Studies

In vitro permeation studies were conducted at 37°C using horizontal, water-jacketed, side-by-side cells (PermeGear Inc., Riegelsville, PA). The tissue was mounted between donor and receiver chambers followed by equilibration with phosphate buffer solution (pH 6.8 in donor and pH 7.4 in receiver) for 30 min. A pH of 6.8 was used in the donor as it represents a mean value of the physiological oral cavity pH (5). The receiver pH was fixed at 7.4 to simulate *in vivo* plasma pH. After the equilibration period, the donor contents were replaced with drug solution in phosphate buffer, pH 6.8 (saturated or sub-saturated depending on drug solubility). Samples were withdrawn from the receiver chamber at different time points and analyzed using HPLC. The donor and receiver contents were stirred with magnetic stir bars to minimize unstirred water layers in the vicinity of the mucosal barrier.

The apparent permeability coefficient, K_p (cm/s) was calculated from the permeation studies using the following equation:

$$K_p = \frac{J_{ss}}{3,600 \times C} = \frac{\Delta Q/\Delta t}{3,600 \times A \times C} \quad (1)$$

where, J_{ss} is the steady-state flux ($\mu\text{g}/\text{h}/\text{cm}^2$), $\Delta Q/\Delta t$ is the steady-state rate of appearance of the drug in the receiver chamber ($\mu\text{g}/\text{h}$), A is the diffusional area (cm^2), and C is the initial drug donor concentration ($\mu\text{g}/\text{mL}$). All permeation studies were conducted in triplicate.

Statistical Analysis

Multiple linear regression (MLR) was performed using NCSS software (NCSS 2000, UT, USA). The molecular descriptors and experimentally determined $\log K_p$ were used as predictor and response variables, respectively during analysis. The various statistical parameters used to evaluate the model include coefficient of determination (R^2), adjusted R^2 , F -ratio and Q^2 (30). R^2 is an indicator of how well the model fits the data. Addition of variables to a regression equation improves R^2 even in the absence of significant predictive capability. The adjusted R^2 avoids this difficulty as it is adjusted for the degrees of freedom (31). Upon addition of variables to an equation, adj. R^2 improves only if the new variables have an additional significant predictive capability. F -ratio is defined as the ratio of regression mean square and residual mean square. Q^2 is the leave-one-out (LOO) cross-validated coefficient of determination. Calculation of this parameter involves omission of one observation and estimation of a regression model using the remaining data points. The equation obtained is then used to predict the response variable for the omitted data point. The correlation between the predicted and observed values in the newly generated data set is used to judge the fit. Q^2 reflects the prediction ability of the model. It can be used to validate the model without selecting another sample or splitting the data (31).

The models were refined through stepwise (step-down or backward) selection of the variables, which involved the permanent removal of a variable that upon exclusion resulted in a better predictive model (higher Q^2) (32). This was repeated until no further improvement was obtained. The minimum root mean square error (RMSE) change value was set at 0.015 so that the stepwise procedure stopped when the maximum relative decrease in the RMSE brought about by changing the status of a variable is less than this amount. The significance levels required for a variable to enter the equation and to be removed from the equation were set at 0.05 and 0.20, respectively. Residual analysis and goodness of fit statistics were performed using S-Plus 4.5.

HPLC Analysis

HPLC methods were developed for all the drugs. The analytical methods were specific for the drug i.e., the drug peak was separated from peaks produced by the solvent and other impurities eluting out of the buccal tissue. The apparatus used for the HPLC analysis was a Waters system (MA, USA) equipped with a Waters 510 pump, Waters 717 plus autosampler, and a Shimadzu SPD-10A UV-Vis detector (Kyoto, Japan). The column used was either a Zorbax SB-C₁₈ column (4.6×150 mm) (Agilent Technologies, Santa Clara, CA) or ODS-AQ C₁₈ (4.6×150 mm; YMC Brand, Waters, MA) depending on the drug. The column was maintained at room temperature (25±2°C). The mobile phase contained a mixture of 50 mM monobasic potassium phosphate (adjusted to pH 3.0 with phosphoric acid), acetonitrile, and methanol. The flow rate was set at 1.0 mL/min. The chromatographic conditions used for analyzing the different drugs are given in Table II.

Table II. Chromatographic Conditions for the Analysis of Various Drugs

Drug	Mobile phase ^a	Column ^b	λ (nm)	Retention time (min)
Nimesulide	60 A+40 B	1	300	5.1
Furosemide	40 A+60 B	2	232	6.9
Naproxen	60 A+40 B	1	224	5.7
Warfarin	60 A+40 B	1	210	7.2
Caffeine	20 A+80 B	1	274	4.5
Antipyrine	25 A+75 B	1	254	4.9
Lidocaine	25 A+75 B	1	224	4.8
Propranolol	40 A+60 B	1	224	5.7
Atenolol	10 A+90 B	2	224	5.3
Metoprolol	30 A+70 B	1	224	5.0
Pindolol	20 A+80 B	1	263	5.3
Bupivacaine	45 A+55 B	1	220	4.5
Verapamil	50 A+50 B	1	235	5.3
Diltiazem	50 A+50 B	1	237	3.7
Amitriptyline	50 A+50 B	1	252	6.6

^a Mobile phase consisted of a mixture of A—acetonitrile+methanol (50/50) and B—50 mM KH₂PO₄ (pH 3.0) buffer

^b HPLC Column: 1—C₁₈ (Zorbax; 4.6×150 mm; Agilent) and 2—ODS-AQ (YMC Brand; 4.6×150 mm; Waters)

RESULTS AND DISCUSSION

Buccal Permeability of Model Drugs

The apparent permeability coefficients (K_p) for the 15 drugs covering a wide range of molecular descriptors were experimentally determined. Out of the 15 drugs, nimesulide ($K_p=30\times 10^{-6}$ cm/s) had the highest permeability while furosemide ($K_p=3.3\times 10^{-9}$ cm/s) had the lowest permeability (Table III) i.e., the permeability of the most permeable drug was 10^4 fold greater than that of the least permeable drug. These permeability values were then used to determine the predictive ability of an existing Potts–Guy (PG) model and in the development of a specific buccal model.

Evaluation of PG Model in the Prediction of Buccal Permeability

The observed permeability values were compared with those predicted using the PG equation (10):

$$\log K_p(\text{cm/s}) = -6.3 + 0.71(\log P) - 0.0061(\text{MW}). \quad (2)$$

A poor correlation ($R^2=0.166$) was observed when the PG model was used to predict the buccal permeability values (Fig. 2). Also, the regression line (solid line) does not overlap the line of identity (dashed line). This analysis clearly demonstrates the limitations of applying the PG model to permeability across buccal membrane and also justifies the development of a new model that is more specific to this tissue. The PG model considers only the lipophilicity parameter ($\log P$) and size (MW). As buccal mucosa has more polar lipids such as phospholipids and glycosylceramides than skin (33), the contribution of the intercellular aqueous pathway to drug permeation is expected to be more. As a result, additional descriptors need to be considered to account for this pathway. In addition, based on the observation that the ionized drug form has significant buccal permeability, the permeation of this form cannot be neglected (34). As the PG model does not consider permeability of the ionized drug form, it is hypothesized that using this model in the buccal field might result in poor prediction. A model, which considers drug

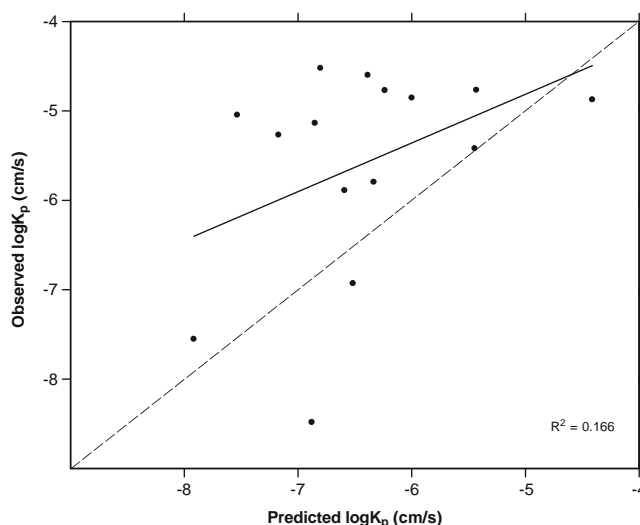


Fig. 2. Correlation between observed and predicted $\log K_p$ values using the PG model.

ionization and ionized form permeability would be more appropriate. Upon replacing the $\log P$ and MW with $\log D_{6,8}$ and MV, respectively, the correlation between the observed and predicted $\log K_p$ improved significantly ($R^2=0.748$). This is in agreement with previous studies, which demonstrate that distribution coefficient is a better indicator than partition coefficient as the former considers drug ionization in addition to the lipophilicity (35). Moreover, using $\log P$ alone to predict permeability is not effective as it models drug absorption only by the passive transcellular route. Also, MV is a better indicator for molecular size than MW (36).

Development of a Predictive Model for Buccal Permeability

Multiple regression using least square estimation was performed on the data set with $\log K_p$ as the dependent variable and the descriptors as predictor variables. Solubilities for atenolol, metoprolol, and pindolol were not determined due to their extremely high values. Stepwise regression using the remaining 12 drugs showed that solubility was not an important descriptor. This descriptor was therefore excluded from subsequent analyses.

Stepwise MLR analysis of buccal permeability with the various descriptors resulted in the following model:

$$\begin{aligned} \log K_p(\text{cm/s}) = & -3.13(\pm 0.95) - 0.0128(\pm 0.0051) \times \text{MV} \\ & - 0.617(\pm 0.170) \times \text{HBD} \\ & + 0.263(\pm 0.110) \times \text{nRotB} \\ & + 0.654(\pm 0.200) \times \log D_{6,8}. \end{aligned} \quad (3)$$

The 95% confidence limits for each regression coefficient are given in parentheses. MV, $\log D_{6,8}$, HBD, and nRotB were found to be the most significant predictor variables. A model including TPSA, HBA and mp along with MV, HBD, nRotB and $\log D_{6,8}$ had a 'probability of a greater t ratio' occurring by chance ($\text{Prob} > |t|$) greater than 0.20 for TPSA, HBA and mp. Descriptors such as TPSA, HBA and mp were therefore not statistically significant. However, the four descriptors—

Table III. Buccal Permeability of Model Drugs

Drug	K_p (cm/s) ^a
Nimesulide	$(30.0 \pm 6.9) \times 10^{-6}$
Furosemide	$(3.3 \pm 0.4) \times 10^{-9}$
Naproxen	$(3.8 \pm 0.3) \times 10^{-6}$
Warfarin	$(1.6 \pm 0.2) \times 10^{-6}$
Caffeine	$(9.0 \pm 0.5) \times 10^{-6}$
Antipyrine	$(5.4 \pm 0.9) \times 10^{-6}$
Lidocaine	$(17.0 \pm 1.8) \times 10^{-6}$
Propranolol	$(14.0 \pm 1.7) \times 10^{-6}$
Atenolol	$(28.0 \pm 3.1) \times 10^{-9}$
Verapamil	$(25.0 \pm 3.6) \times 10^{-6}$
Diltiazem	$(7.3 \pm 0.7) \times 10^{-6}$
Amitriptyline	$(13.0 \pm 1.8) \times 10^{-6}$
Bupivacaine	$(17.0 \pm 1.1) \times 10^{-6}$
Metoprolol	$(1.3 \pm 0.2) \times 10^{-6}$
Pindolol	$(12.0 \pm 0.9) \times 10^{-8}$

^a K_p is given as (mean \pm SD) of triplicate samples

MV, $\log D_{6,8}$, HBD, and nRotB, were found to influence permeability significantly with a ($\text{Prob} > |t|$) less than 0.001. An excellent fit with a coefficient of determination adjusted for degrees of freedom (adj. R^2) of 0.946 was obtained (Fig. 3). Also, the regression line overlapped the line of identity. The predictability of the model was good based on a Q^2 value of 0.882. In addition, the histograms of the residuals were found to be normally distributed with a mean of zero (Fig. 4) suggesting that the normality assumption of the error term is likely met (37). Estimates of the parameters were also obtained using maximum likelihood estimation (MLE) (NONMEM Version V, Level 1.1). The objective of MLE is to select values for parameters that maximize the likelihood function i.e., to seek a probability distribution that makes the observed data most likely (38). MLE allows the use of each individual data point rather than the mean of drug permeability. This increases the sample size to 45 from 15 (permeation studies were performed as triplicate). The parameters obtained using MLE were similar to those obtained using MLR. In addition, the $Q-Q$ (quantile-quantile) plot of the residuals showed that all points lie close to a straight line (Fig. 4). Residual analysis performed on the data revealed a random, symmetric scattering of points about zero. A line drawn using locally weighted regression smoothing (LOESS) passed through the origin and had a slope of almost zero (Fig. 4). These results show the appropriateness of the developed model and validity of its basic assumptions and also support the model estimated using MLR.

Drug permeability across biological membranes such as skin, intestine, and the blood brain barrier (BBB) is widely known to increase with permeant lipophilicity and decrease with molecular size (11). It is therefore not surprising that both $\log D_{6,8}$ and MV are important in governing the permeability across the buccal mucosa as well. However, in addition to these descriptors, HBD and nRotB were also found to be important in predicting buccal permeability. Previous studies have demonstrated that a greater hydrogen bonding capability, especially, the number of hydrogen bond donors, of a molecule decreases its permeability probably

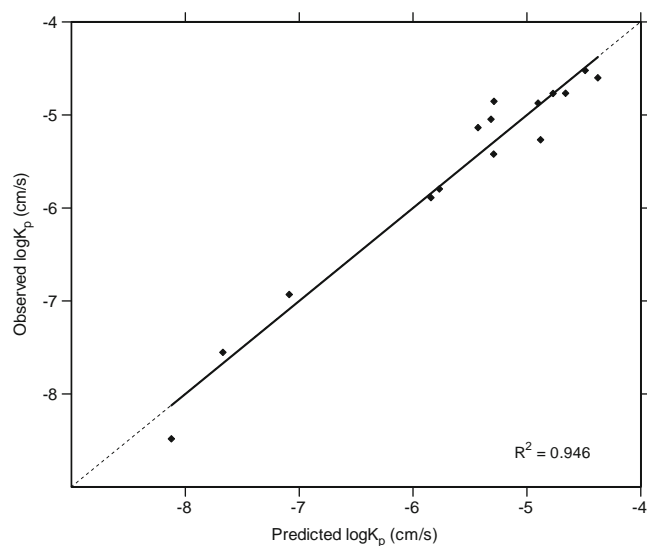


Fig. 3. Correlation between observed and predicted $\log K_p$ values using the buccal model.

due to increased interactions with the lipid bilayer (14,39). In an earlier study by Winiwarter *et al.*, the human jejunal permeability values of 13 passively absorbed compounds were correlated with several physicochemical descriptors using partial least squares (PLS) (40). The best model reported by these researchers consisted of $\log D_{5,5}$, PSA and HBD. Another study by Linnankoski *et al.* also revealed that HBD (and not HBA) was among the most important parameters describing the oral absorption rate constant (39). The reason for the importance of HBD in permeability might be the predominant presence of hydrogen bond acceptors in the head group regions of membrane bilayer lipids (11). As a result, the permeability of solutes with significant hydrogen bonding donor tendencies is restricted (41,42). The presence of nRotB in the model indicated that a greater flexibility of a molecule favors buccal permeation. Hou *et al.* obtained a better correlation between Caco-2 permeability and molecular properties when descriptors related to molecular flexibility were introduced in the analysis (36).

RMSE, which is an estimate of the standard deviation of the residuals, was 0.274 and 1.700 in case of the buccal and PG models, respectively. This shows that the buccal model has better precision and bias than the PG model. Also, the buccal model fit the data better and had a better permeability prediction than the PG model.

Validation Using an External Data Set

An external test set compiled from data reported in literature was used to challenge the buccal model developed in the previous section. The external data set was restricted to small molecules. Only studies involving tissues with thickness in the range of 400–750 μ were considered. Heat-separated epithelia were also included as one study reported the thickness of the heat-separated tissue to be 410 μ (43). The permeabilities for the following compounds were obtained from literature: sotalol, flecainide, morphine, zalcitabine, fentanyl, thiocolchicoside, nicotine, estradiol, triamcinolone acetonide, testosterone, labetalol, acebutolol, timolol, oxprenolol, alprenolol, and tertatolol (43–51). Sotalol was excluded as it has a $\log D_{6,8}$ of -2.59 , which is lower than that of atenolol, the most hydrophilic compound ($\log D_{6,8} = -1.3$) in the training group used in developing the model (16). Similarly, thiocolchicoside has a MW (564 Da), HBA (11) and PSA (164 \AA^2) beyond the range of the molecules included in the model development and was therefore, not included. Zalcitabine was not included as a 14-fold difference in permeability was observed in two different studies (44,45). The permeability of nicotine across a buccal mucosa with mean thickness of 736 μ was reported to be 1.5×10^{-8} cm/s at pH 7.4 by Nielsen *et al.* (49). However, another study performed by Squier *et al.* resulted in a much higher K_p of 5.6×10^{-7} cm/s at pH 7.5 (52). In addition, Squier *et al.* performed permeability studies across full-thickness mucosa (with a thickness greater than 736 μ ; value not reported). A thinner tissue with a thickness around 700 μ is expected to result in a greater permeability. Also, the *in vivo* buccal permeability of this compound (at pH 7.4) was reported to be 2.1×10^{-4} cm/s, which is about 14,000 times greater than the *in vitro* permeability (53). All these factors point to a discrepancy in the buccal permeability of nicotine. As a

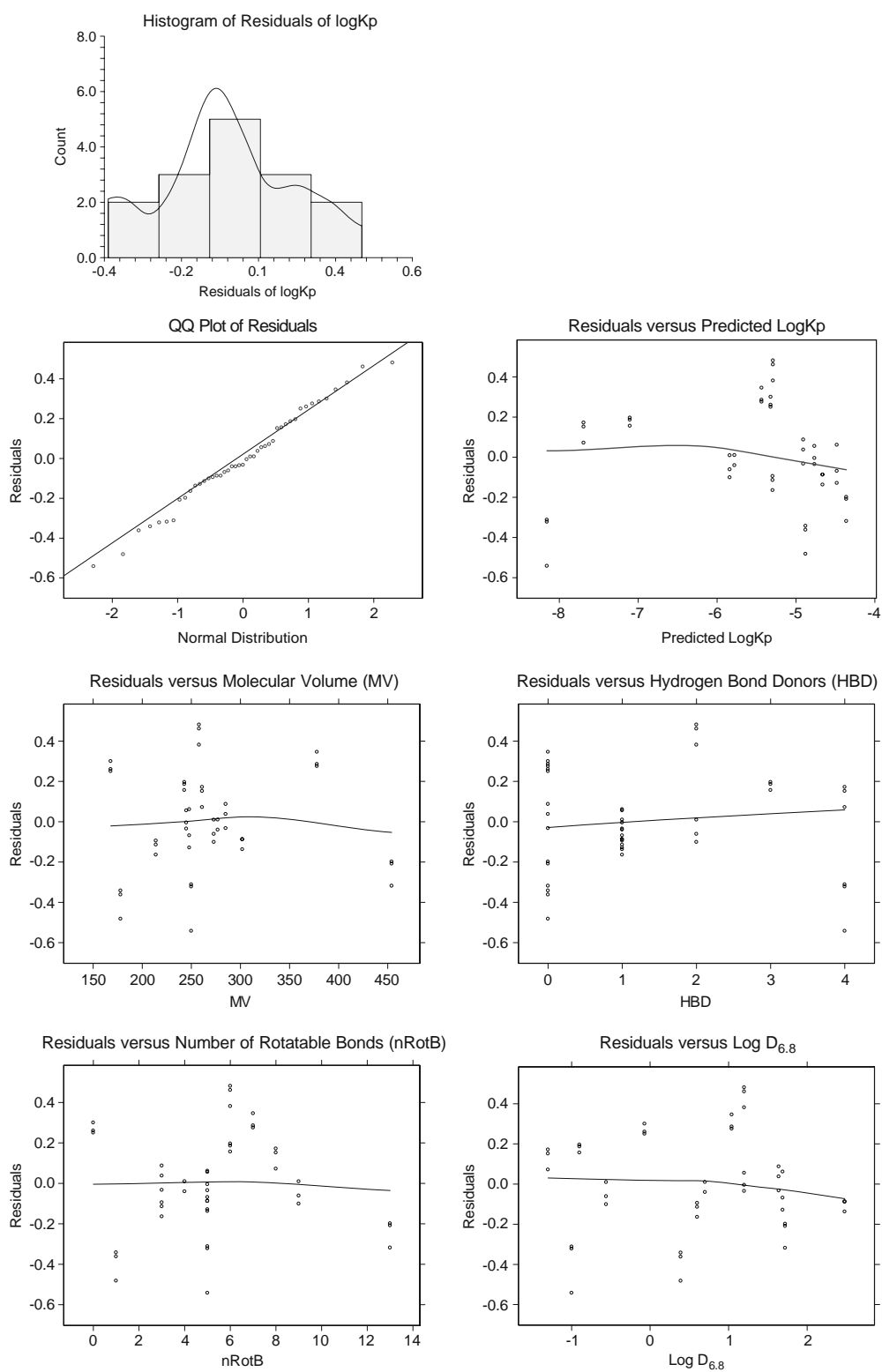


Fig. 4. Goodness of fit statistics for the buccal model.

result, this compound was not considered for external validation of the model.

The remaining 12 compounds along with the in-house permeability value for bupropion were considered. The descriptors, observed $\log K_p$, predicted $\log K_p$ and the difference between the observed and predicted $\log K_p$ (residual) for

these 13 compounds is given in Table IV. Most of the compounds had a residual within the range -1.0 to $+1.0$ i.e., the ratio of observed K_p and predicted K_p was within 0.1 to 10. The two outliers were morphine and triamcinolone acetonide. Molecules with a complex fused ring structure like atropine and etorphine (a morphine analogue) were found to

Table IV. External Validation of the Buccal Model

Drug	Observed $\log K_p$ (cm/s)	MV	HBD	nRotB	$\log D_{6.8}$	Predicted $\log K_p$ (cm/s)	Residual	Ref.
Buspirone	-4.81	371	0	6	2.8 ^a	-4.58	-0.24	In-house
Flecainide ^b	-7.19	332	2	9	0.05	-6.31	-0.88	(46)
Morphine	-5.72	257	2	0	-0.7	-8.17	2.44	(48)
Fentanyl	-5.15	340	0	6	1.41	-5.07	-0.08	(43)
Labetalol	-7.70	315	5	8	-0.03	-8.26	0.57	(51)
Acebutolol	-7.40	331	3	10	-1.56	-7.71	0.31	(51)
Timolol	-6.52	291	2	7	-1.71	-7.44	0.92	(51)
Oxprenolol	-5.52	267	2	9	-0.81	-6.03	0.50	(51)
Alprenolol	-5.70	258	2	8	-0.26	-5.81	0.11	(51)
Tertatolol	-6.00	288	2	6	-0.37	-6.79	0.79	(51)
Testosterone	-5.96	292	1	0	3.32	-5.39	-0.57	(51)
Estradiol	-4.54	269	2	0	4.01	-5.26	0.71	(50)
Triamcinolone acetonide	-5.55	390	2	2	2.53	-7.28	1.73	(50)

$\log D_{6.8}$ for the drugs was obtained using ChemIDplus (16)

^a From ref. (29)

^b K_p of flecainide was calculated from the flux and concentration

be outliers in transdermal models (54). Morphine due to its complex fused ring structure might behave similarly in the buccal mucosa. In case of steroids, permeation studies across skin have revealed several molecules belonging to this group to be significant outliers (55). The three different steroids in the external set for this study were estradiol, testosterone, and triamcinolone acetonide. Surprisingly, transdermal studies in literature have not reported estradiol and testosterone as outliers. Steroids are known to alter the fluidity of biological membranes. Also, the pharmacological action of hydrophilic steroids is linked to changes in membrane fluidity (56). As triamcinolone acetonide is more hydrophilic than estradiol and testosterone, the alteration in fluidity might be greater too, thereby resulting in an increased permeation. It is also possible that the model does not consider an important descriptor that governs the permeability of certain steroids.

An overlap of the external data set (without morphine, but including triamcinolone acetonide) on the permeability values obtained using the model is given in Fig. 5. A good correlation ($R^2=0.636$) was obtained between the observed and predicted $\log K_p$ values (using the buccal model) for this data set. The PG model resulted in a poor correlation ($R^2=0.191$) for the external data set. It should be noted that as the data was obtained from different literature sources, it is inevitable that a high degree of experimental error owing to inter-laboratory variability is involved. Despite this restriction, the buccal permeability model reported here was able to predict the permeabilities of most of the compounds within a reasonable error range. Also, this model was able to take into account a wide range of descriptors for the drugs in the external data set. The various descriptors (excluding nicotine, morphine, and triamcinolone acetonide) ranged from 258 to 371 (MV), 0 to 5 (HBD), 0 to 10 (nRotB), and -1.71 to 4.01 ($\log D_{6.8}$). In addition, the $\log K_p$ values ranged from -8.26 to -4.58.

To our knowledge, this is the first attempt at predicting buccal permeability. This simple computational method is suitable for screening drug and drug-like compound libraries for their suitability to delivery through buccal route. Also, the *in silico* model described in this work can contribute to early strategy and decision making while selecting and developing

drugs for buccal delivery. Based on the predicted permeability value, the intended drug concentration and the area of the drug delivery system, the predicted rate of transport may be calculated. This value can be compared with the target rate of drug administration, which is given as a product of the total body clearance (TBC) and minimum effective concentration (MEC) (44). If the target rate of administration is significantly greater than the predicted rate of administration, a decision can be made either on the modification of the drug formulation pH or the use of an appropriate permeation enhancer along with the drug.

It is also believed that as more data becomes available, it can be added to the existing data to refine the model. The addition of more drugs would increase the structural complexity considered and thereby, increase the predictive ability of the model.

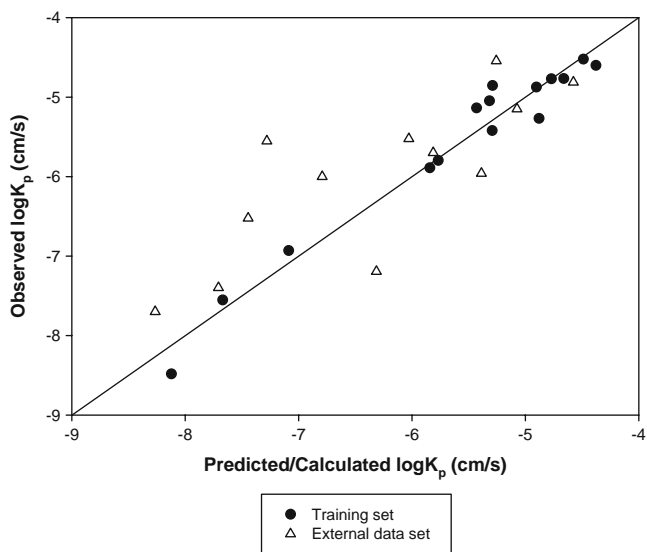


Fig. 5. External test set (12 drugs) overlapped on the $\log K_p$ values for the 15 drugs used in this study.

CONCLUSION

A computational model to predict buccal permeability of drugs based on their structural and physicochemical properties was developed. Molecular volume, $\log D_{6,8}$, number of hydrogen bond donors, and number of rotatable bonds were the most important parameters describing $\log K_p$.

The predictive capability of the buccal model was better than the existing models that describe permeation across skin, which is distinctly different from buccal epithelium. The final model was also challenged with an external data set consisting of permeability values from the literature. Considering the huge inter-laboratory variation in the experimental protocols as well as the variability in drug descriptors in the external set, the model was able to reasonably predict permeabilities for most of the drugs from the external data set.

REFERENCES

- M. Rathbone, B. Drummond, and I. Tucker. The oral cavity as a site for systemic drug delivery. *Adv. Drug Del. Rev.* **13**:1–22 (1994). doi:10.1016/0169-409X(94)90024-8.
- W. R. Galey, H. K. Lonsdale, and S. Nacht. The *in vitro* permeability of skin and buccal mucosa to selected drugs and tritiated water. *J. Invest. Dermatol.* **67**:713–717 (1976). doi:10.1111/1523-1747.ep12598596.
- C. A. Squier, and P. W. Wertz. Permeability and pathophysiology of oral mucosa. *Adv. Drug Deliv. Rev.* **12**:13–24 (1993). doi:10.1016/0169-409X(93)90038-6.
- A. Kokate, V. Marasanapalle, B. R. Jasti, and X. Li. Physiological and biochemical barriers to drug delivery. In B. R. Jasti (ed.), *Design of controlled release drug delivery systems*, McGraw-Hill, New York, 2006, p. 41.
- P. P. H. Le Brun, P. L. A. Fox, M. E. de Vries, and H. E. Bodde. *In vitro* penetration of some β -adrenoreceptor blocking drugs through porcine buccal mucosa. *Int. J. Pharm.* **49**:141–145 (1989). doi:10.1016/0378-5173(89)90113-0.
- Y. Sudhakar, K. Kuotsu, and A. K. Bandyopadhyay. Buccal bioadhesive drug delivery—a promising option for orally less efficient drugs. *J. Control. Release.* **114**:15–40 (2006). doi:10.1016/j.jconrel.2006.04.012.
- C. A. Squier, P. Cox, and P. W. Wertz. Lipid content and water permeability of skin and oral mucosa. *J. Invest. Dermatol.* **96**:123–126 (1991). doi:10.1111/1523-1747.ep12515931.
- P. W. Wertz, and C. A. Squier. Cellular and molecular basis of barrier function in oral epithelium. *Crit. Rev. Ther. Drug Carrier Syst.* **8**:237–269 (1991).
- C. A. Lesch, C. A. Squier, A. Cruchley, D. M. Williams, and P. Speight. The permeability of human oral mucosa and skin to water. *J. Dent. Res.* **68**:1345–1349 (1989).
- R. O. Potts, and R. H. Guy. Predicting skin permeability. *Pharm. Res.* **9**:663–669 (1992). doi:10.1023/A:1015810312465.
- A. Malkia, L. Murtomaki, A. Urtti, and K. Kontturi. Drug permeation in biomembranes: *in vitro* and *in silico* prediction and influence of physicochemical properties. *Eur. J. Pharm. Sci.* **23**:13–47 (2004). doi:10.1016/j.ejps.2004.05.009.
- Molinspiration. <http://www.molinspiration.com> (2007).
- P. Ertl, B. Rohde, and P. Selzer. Fast calculation of molecular polar surface area as a sum of fragment-based contributions and its application to the prediction of drug transport properties. *J. Med. Chem.* **43**:3714–3717 (2000). doi:10.1021/jm000942e.
- D. F. Veber, S. R. Johnson, H. Y. Cheng, B. R. Smith, K. W. Ward, and K. D. Kopple. Molecular properties that influence the oral bioavailability of drug candidates. *J. Med. Chem.* **45**:2615–2623 (2002). doi:10.1021/jm020017n.
- C. A. Bergstrom, K. Luthman, and P. Artursson. Accuracy of calculated pH-dependent aqueous drug solubility. *Eur. J. Pharm. Sci.* **22**:387–398 (2004). doi:10.1016/j.ejps.2004.04.006.
- ChemIDplus. <http://chem.sis.nlm.nih.gov/chemidplus/> (2007).
- J. Hadgraft, and C. Valenta. pH, pK(a) and dermal delivery. *Int. J. Pharm.* **200**:243–247 (2000). doi:10.1016/S0378-5173(00)00402-6.
- K. Fredholt, D. H. Larsen, and C. Larsen. Modification of *in vitro* drug release rate from oily parenteral depots using a formulation approach. *Eur. J. Pharm. Sci.* **11**:231–237 (2000). doi:10.1016/S0928-0987(00)00104-4.
- B. A. Hendriksen, M. V. Felix, and M. B. Bolger. The composite solubility versus pH profile and its role in intestinal absorption prediction. *AAPS Pharm. Sci.* **5**:E4 (2003). doi:10.1208/ps050104.
- J. Jacobsen, B. Van deurs, M. Pedersen, and M. R. Rassing. TR146 cells grown on filters as a model for human buccal epithelium: I. Morphology, growth, barrier properties, and permeability. *Int. J. Pharm.* **125**:165–184 (1995). doi:10.1016/0378-5173(95)00109-V.
- A. Avdeef, P. Artursson, S. Neuhoff, L. Lazorova, J. Grašjo, and S. Tavelin. Caco-2 permeability of weakly basic drugs predicted with the double-sink PAMPA pKa(flux) method. *Eur. J. Pharm. Sci.* **24**:333–349 (2005). doi:10.1016/j.ejps.2004.11.011.
- ACD, Re-evaluation of logP data for 22 drugs and comparison of 6 calculation methods, in: (ACD Labs, 2006).
- F. Yoshida, and J. G. Topliss. QSAR model for drug human oral bioavailability. *J. Med. Chem.* **43**:2575–2585 (2000). doi:10.1021/jm0000564.
- P. Modamio, C. F. Lastra, and E. L. Marino. A comparative *in vitro* study of percutaneous penetration of beta-blockers in human skin. *Int. J. Pharm.* **194**:249–259 (2000). doi:10.1016/S0378-5173(99)00380-4.
- P. R. B. Fallavena, and E. E. S. Schapoval. pKa determination of nimesulide in methanol–water mixtures by potentiometric titrations. *Int. J. Pharm.* **158**:109–112 (1997). doi:10.1016/S0378-5173(97)00221-4.
- F. Akomeah, T. Nazir, G. P. Martin, and M. B. Brown. Effect of heat on the percutaneous absorption and skin retention of three model penetrants. *Eur. J. Pharm. Sci.* **21**:337–345 (2004). doi:10.1016/j.ejps.2003.10.025.
- K. Higaki, M. Asai, T. Suyama, K. Nakayama, K. Ogawara, and T. Kimura. Estimation of intradermal disposition kinetics of drugs: II. Factors determining penetration of drugs from viable skin to muscular layer. *Int. J. Pharm.* **239**:129–141 (2002). doi:10.1016/S0378-5173(02)00084-4.
- Merck. *Merck Index*, New Jersey, 1976.
- R. Birudaraj, B. Berner, S. Shen, and X. Li. Buccal permeation of buspirone: mechanistic studies on transport pathways. *J. Pharm. Sci.* **94**:70–78 (2005). doi:10.1002/jps.20208.
- S. Geinoz, R. H. Guy, B. Testa, and P. A. Carrupt. Quantitative structure-permeation relationships (QSPeRs) to predict skin permeation: a critical evaluation. *Pharm. Res.* **21**:83–92 (2004). doi:10.1023/B:PHAM.0000012155.27488.2b.
- NCCS, *User's Guide: Regression and curve fitting*, NCCS, Kaysville, Utah, 2006.
- C. A. Bergstrom, C. M. Wassvik, U. Norinder, K. Luthman, and P. Artursson. Global and local computational models for aqueous solubility prediction of drug-like molecules. *J. Chem. Inf. Comput. Sci.* **44**:1477–1488 (2004). doi:10.1021/ci049990h.
- P. W. Wertz, D. C. Swartzendruber, and C. A. Squier. Regional variation in the structure and permeability of oral mucosa and skin. *Adv. Drug Deliv. Rev.* **12**:1–12 (1993). doi:10.1016/0169-409X(93)90037-5.
- A. Kokate, X. Li, P. Singh, and B. R. Jasti. Effect of thermodynamic activities of the unionized and ionized species on drug flux across buccal mucosa. *J. Pharm. Sci.* **97**:4294–4306 (2008). doi:10.1002/jps.21301.
- P. Artursson, K. Palm, and K. Luthman. Caco-2 monolayers in experimental and theoretical predictions of drug transport. *Adv. Drug Deliv. Rev.* **46**:27–43 (2001). doi:10.1016/S0169-409X(00)00128-9.
- T. J. Hou, W. Zhang, K. Xia, X. B. Qiao, and X. J. Xu. ADME evaluation in drug discovery. 5. Correlation of Caco-2 permeation with simple molecular properties. *J. Chem. Inf. Comput. Sci.* **44**:1585–1600 (2004). doi:10.1021/ci049884m.
- M. J. Campbell. *Statistics at square two: Understanding modern statistical applications in medicine*. BML Publishing Group, London, 2001.
- I. Jae Myung. Tutorial on maximum likelihood estimation. *J. Math. Psychol.* **47**:90–100 (2003). doi:10.1016/S0022-2496(02)00028-7.

39. J. Linnankoski, J. M. Makela, V. P. Ranta, A. Urtili, and M. Yliperttula. Computational prediction of oral drug absorption based on absorption rate constants in humans. *J. Med. Chem.* **49**:3674–3681 (2006). doi:10.1021/jm051231p.
40. S. Winiwarter, N. M. Bonham, F. Ax, A. Hallberg, H. Lennernas, and A. Karlen. Correlation of human jejunal permeability (*in vivo*) of drugs with experimentally and theoretically derived parameters. A multivariate data analysis approach. *J. Med. Chem.* **41**:4939–4949 (1998). doi:10.1021/jm9810102.
41. N. el Tayar, R. S. Tsai, B. Testa, P. A. Carrupt, and A. Leo. Partitioning of solutes in different solvent systems: the contribution of hydrogen-bonding capacity and polarity. *J. Pharm. Sci.* **80**:590–598 (1991). doi:10.1002/jps.2600800619.
42. R. A. Conradi, A. R. Hilgers, N. F. Ho, and P. S. Burton. The influence of peptide structure on transport across Caco-2 cells. II. Peptide bond modification which results in improved permeability. *Pharm. Res.* **9**:435–439 (1992). doi:10.1023/A:1015867608405.
43. I. Diaz Del Consuelo, G. P. Pizzolato, F. Falson, R. H. Guy, and Y. Jacques. Evaluation of pig esophageal mucosa as a permeability barrier model for buccal tissue. *J. Pharm. Sci.* **94**:2777–2788 (2005). doi:10.1002/jps.20409.
44. J. Xiang, X. Fang, and X. Li. Transbuccal delivery of 2',3'-dideoxycytidine: *in vitro* permeation study and histological investigation. *Int. J. Pharm.* **231**:57–66 (2002). doi:10.1016/S0378-5173(01)00865-1.
45. A. H. Shojaei, M. Khan, G. Lim, and R. Khosravan. Transbuccal permeation of a nucleoside analog, dideoxycytidine: effects of menthol as a permeation enhancer. *Int. J. Pharm.* **192**:139–146 (1999). doi:10.1016/S0378-5173(99)00301-4.
46. V. H. Deneer, G. B. Drese, P. E. Roemele, J. C. Verhoef, A. H. L. Lie, J. H. Kingma, J. R. Brouwers, and H. E. Junginger. Buccal transport of flecainide and sotalol: effect of a bile salt and ionization state. *Int. J. Pharm.* **241**:127–134 (2002). doi:10.1016/S0378-5173(02)00229-6.
47. M. Artusi, P. Santi, P. Colombo, and H. E. Junginger. Buccal delivery of thiocolchicoside: *in vitro* and *in vivo* permeation studies. *Int. J. Pharm.* **250**:203–213 (2003). doi:10.1016/S0378-5173(02)00545-8.
48. S. Senel, D. Duchene, A. A. Hincal, Y. Capan, and G. Ponchel. *In vitro* studies on enhancing effect of sodium glycocholate on transbuccal permeation of morphine hydrochloride. *J. Control. Release.* **51**:107–113 (1998). doi:10.1016/S0168-3659(97)00099-0.
49. H. M. Nielsen, and M. R. Rassing. Nicotine permeability across the buccal TR146 cell culture model and porcine buccal mucosa *in vitro*: effect of pH and concentration. *Eur. J. Pharm. Sci.* **16**:151–157 (2002). doi:10.1016/S0928-0987(02)00083-0.
50. J. A. Nicolazzo, B. L. Reed, and B. C. Finnin. Modification of buccal drug delivery following pretreatment with skin penetration enhancers. *J. Pharm. Sci.* **93**:2054–2063 (2004). doi:10.1002/jps.20113.
51. H. M. Nielsen, and M. R. Rassing. TR146 cells grown on filters as a model of human buccal epithelium: IV. Permeability of water, mannitol, testosterone and beta-adrenoceptor antagonists. Comparison to human, monkey and porcine buccal mucosa. *Int. J. Pharm.* **194**:155–167 (2000). doi:10.1016/S0378-5173(99)00368-3.
52. C. A. Squier. Penetration of nicotine and nitrosornicotine across porcine oral mucosa. *J. Appl. Toxicol.* **6**:123–128 (1986). doi:10.1002/jat.2550060211.
53. C. L. Adrian, H. B. Olin, K. Dalhoff, and J. Jacobsen. *In vivo* human buccal permeability of nicotine. *Int. J. Pharm.* **311**:196–202 (2006). doi:10.1016/j.ijpharm.2005.12.039.
54. M. T. Cronin, J. C. Dearden, G. P. Moss, and G. Murray-Dickson. Investigation of the mechanism of flux across human skin *in vitro* by quantitative structure-permeability relationships. *Eur. J. Pharm. Sci.* **7**:325–330 (1999). doi:10.1016/S0928-0987(98)00041-4.
55. H. Patel, W. ten Berge, and M. T. Cronin. Quantitative structure-activity relationships (QSARs) for the prediction of skin permeation of exogenous chemicals. *Chemosphere.* **48**:603–613 (2002). doi:10.1016/S0045-6535(02)00114-5.
56. F. Faassen, J. Kelder, J. Lenders, R. Onderwater, and H. Vromans. Physicochemical properties and transport of steroids across Caco-2 cells. *Pharm. Res.* **20**:177–186 (2003). doi:10.1023/A:1022210801734.